THEORETICAL OPTICAL FLOW FOR TARGET POSITION PREDICTION ON FLS IMAGES

Isabelle Quidu[a], Yann Dupas[b], Luc Jaulin[c]

[a]isabelle.quidu@ensieta.fr
[b]yann.dupas@dga.defense.gouv.fr
[c]luc.jaulin@ensieta.fr

Isabelle QUIDU
ENSIETA / E3I2 laboratory, 2 rue François Verny, 29806 Brest Cedex 9, France
Phone: (33) 2 98 34 89 15, Fax number: (33) 2 98 34 87 50
E-mail : isabelle.quidu@ensieta.fr

Abstract: *This study is related to the obstacle avoidance issue for an Autonomous Underwater Vehicle (AUV). In addition to its original mission, the vehicle must ensure its own survival and therefore understand the environment in safety. The use of a Forward Looking Sonar (FLS) on AUV is one of the most efficient solutions to detect unexpected and potentially dangerous changes of the environment, like the presence of obstacles or seabed slope. Like this, a FLS can prevent the vehicle from obstacles or terrain that may endanger the underwater vehicle. Besides navigation is performed knowing data from a Doppler Velocity Log (DVL) and a Motion Reference Unit (MRU). From these last data a process model has been derived in order to predict the motion of a ground target detected in a sonar image. The state vector is composed of the coordinates of the target in the image. Motion prediction leads to a theoretical optical flow that we can compare to an observed optical flow based on images correlation.*

This study is of high interest for the French organism GESMA which is involved in the development of decisional autonomy for AUV for several years. Results will be given on real data recorded in April 2006 during sea trials organized by GESMA and should be extended on data recorded during future campaigns involving the Rapid Environment Assessment (REA) AUV "Daurade".

Keywords: *Optical flow - Obstacle Detection and Avoidance – AUV – Forward Looking Sonar*

1. INTRODUCTION

The development of AUVs is a real challenge for researchers that have to supply the vehicle with a total autonomy in terms of energy, data processing, navigation in order to enable it to bring off its mission. This leads to related issues such as survival in a hostile context. A Forward Looking Sonar (FLS) can prevent the vehicle from obstacles or terrain that may endanger the underwater vehicle [1]. Indeed by combining imaging data with navigation data, still ground targets can be detected and tracked. The first step of tracking consists in deriving a process model in order to predict the motion of ground targets on the sonar screen. This model will be used in the prediction step of a Kalman filter that will be implemented later to track a still target through the following frames. A theoretical optical flow based on the process model can be visualised on the sonar images sequence and compared to an observed optical flow based on images correlation.

This study is of high interest for GESMA involved in the development of experimental AUVs such as the Redermor for several years [2] [3] and more recently in the Rapid Environment Assessment (REA) AUV "Daurade" [4].

This paper has been divided into three main parts. Part number 2 gives a quick description of data at our disposal in this study. The development of part 3 ends with the process model able to predict the motion of a target detected on the sonar screen by taking into account navigation data. The fourth part gives some results on real data.

2. DATA DESCRIPTION

2.1. Sea trials

The *Redermor* is the experimental platform deployed from the French Navy ship *BEGM Thetis*. It is a heavy and large AUV (3.8 tons x 6 m).

In order to test the capability of the *Redermor* vehicle to react when obstacles are encountered on its way, GESMA organized an experimental trial in April 2006, named DEVITOBS'06 "DETection et EVITement d'OBStacles". The aim of this campaign was to record sonar data in several modes with various obstacles. In that way, it has been possible to test, qualify and upgrade the sensors suite, to initiate an obstacle database, to start algorithm development on those obstacles. The goal was to prepare avoidance tactics and strategies to be given to robot mission supervisor.

The experiment has been conducted in the Douarnenez Bay, near Brest. Several objects have been laid: a moored mine like object, a net and plastic chains. Other objects have been investigated like the shipwreck "Meuse" in the same bay and schools of fish. Up to now analysis has been mainly focussed on the Reson 8101 data.

2.2. Avoidance sonar data

In its last release, avoidance means of Redermor consist of a network of 10 *Tritech* echosounders and a *Reson Seabat 8101* Forward Looking Sonar. The 240 kHz *Reson Seabat 8101* FLS is derived from a multibeam echosounder and can operate in bathymetric mode or a sector scan mode. The system integrated in the Redermor can play a beamformed image over a 15° (vertical) x 60° (horizontal) sector with a 1.5° azimuth resolution and a 5 cm range resolution. The sonar has been oriented 15° from the horizontal plane.

In this article sonar data used only come from the *Reson Seabat 8101* FLS. The *Reson Seabat 8101* FLS provides data that are processed and plotted on a sector Plan Position Indicator (PPI) display. This image is characterized by low contrast. The receive beam of 1.5° (H) by 15° (V) does not provide precise details and precise localization of the obstacle. For a range from 20 to 100m, the resolution cell increases from about 50cm to 2.5m in length according to the sector formed.

2.3. Navigation data

Navigation is performed knowing data from a Doppler Velocity Log (DVL) and a Motion Reference Unit (MRU). The DVL gives the vehicle speed in relation to the seafloor. The MRU gives the vehicle orientation and its acceleration in relation to the earth (or absolute) reference frame (X : geographical North, Y : East, Z : gravity direction).

In the AUV environment, one can consider the absolute reference frame $R_a(\mathbf{O_a,i_a,j_a,k_a})$ where the $\mathbf{i_a}$ vector stands for geographical North, $\mathbf{j_a}$ stands for East and $\mathbf{k_a}$ is oriented towards the centre of the Earth, $\mathbf{O_a}$ is a point at the ocean surface. Besides, let us consider the AUV (or mobile) reference frame $R_r(\mathbf{O_r,i_r,j_r,k_r})$ where $\mathbf{O_r}$ is merged with the inertia centre of the vehicle, $\mathbf{i_r}$ is oriented towards the front of the vehicle, $\mathbf{k_r}$ towards the seafloor and $\mathbf{j_r}$ direction is deduced from $\mathbf{i_r}$ and $\mathbf{k_r}$ to provide an orthonormal reference frame (see Fig. 1).

To convert the coordinates from the mobile reference frame to the absolute reference frame we use a rotation matrix $R_{Euler}(\varphi,\theta,\psi)$ where (φ,θ,ψ) are the Euler angles. The angles provided by the MRU are sufficient to describe any vehicle motion.

In the absolute reference frame, the following data are available :

$\boldsymbol{p}_a = \left(p_a^x, p_a^y, p_a^z\right)$ stands for the coordinates of the AUV (we supposed its location merged with all the other sensors)

$\boldsymbol{m}_a = \left(m_a^x, m_a^y, m_a^z\right)$ stands for the coordinates of an object laying on the seafloor

$\boldsymbol{v}_a = \left(v_a^x, v_a^y, v_a^z\right)$ stands for the speed of the AUV

In the mobile reference frame, the following data are available :

$\boldsymbol{v}_r = \left(v_r^x, v_r^y, v_r^z\right)$ stands for the speed of the AUV (measured by the DVL)

$\boldsymbol{m}_r = \left(m_r^x, m_r^y, m_r^z\right)$ stands for the coordinates of an object laying on the seafloor

3. PROCESS MODEL [5][6]

3.1. Introduction

The researched process model must describe the motion of a target whose coordinates are (x_e, y_e) on the sonar screen given the navigation data. This model is obtained in two steps :

- The first one consists in modelling the coordinate conversion from the mobile reference frame to the screen image reference frame. In other words, it consists in finding the relation between the sonar coordinates (d, δ) of the target in the

mobile reference frame and the screen coordinates (x_e, y_e). Let us call g the corresponding function.

- The second one consists in modelling the motion of the target on the screen by taking into account the navigation data. Let us call f the corresponding function. We have $\dot{p}_e = (\dot{x}_e, \dot{y}_e) = f(x_e, y_e, \boldsymbol{u}) = f(p_e, \boldsymbol{u})$, where $\boldsymbol{u}$ stands for a vector of navigation data.

Fig. 1 gives the operational configuration with the position of variables used in the following. Seafloor is supposed to be flat.
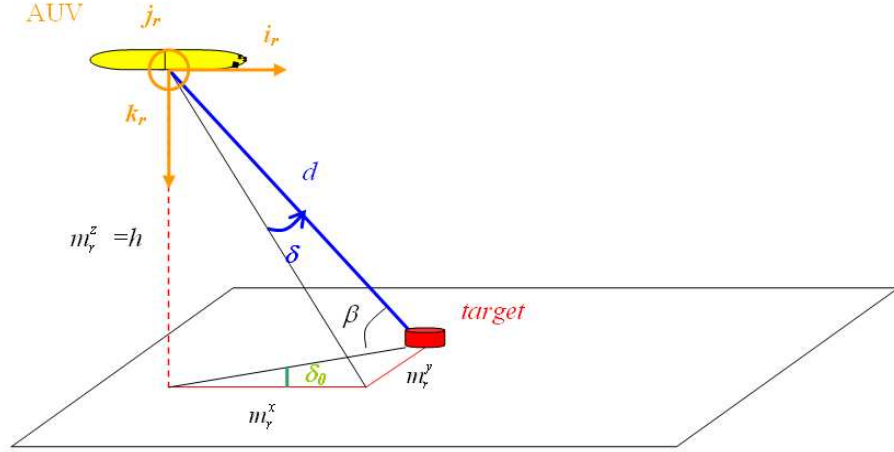

Fig.1: operational configuration

3.2. First step

In order to visualise a sector image, we have to convert polar data to Cartesian data given the following equations:

$$\begin{cases} x = r \times \sin\theta & \text{along the columns} \\ y = r \times \cos\theta & \text{along the rows} \end{cases} \quad \text{with} \quad \begin{cases} r = d / \Delta d \\ \theta = \delta / \Delta\theta \end{cases} \tag{1}$$

where
(r, θ) stand for polar coordinates
(x, y) stand for Cartesian coordinates
(d, δ) stand for sonar coordinates (distance, azimuth)
$(\Delta d, \Delta\theta)$ stand for sampling rates in range and in azimuth

Finally, to follow the image representation norm of MatLab (image whose size is M rows by N columns), a reference frame rotation is operated to convert Cartesian sonar coordinates (x, y) into Cartesian screen coordinates (x_e, x_e) such as:

$$\begin{cases} \delta = \Delta\theta \times \arctan\left(\dfrac{-x_e + \dfrac{N}{2}}{-y_e + M}\right) \\[4em] d = \Delta d \dfrac{-x_e + \dfrac{N}{2}}{\sin\left[\arctan\left(\dfrac{-x_e + \dfrac{N}{2}}{-y_e + M}\right)\right]} \end{cases} \tag{2}$$

Or, $\begin{cases} x_e = \dfrac{N}{2} - \dfrac{d}{\Delta d}\sin\left(\dfrac{\delta}{\Delta\theta}\right) \\ y_e = M - \dfrac{d}{\Delta d}\cos\left(\dfrac{\delta}{\Delta\theta}\right) \end{cases}$ i.e. $(x_e, y_e) = g(d, \delta)$ (3)

This first step allows conversion from the mobile reference frame to the image reference frame.

3.3. Second step

The model of the vehicle is given by:

$$\dot{\boldsymbol{p}}_a = \boldsymbol{v}_a = R_{euler}(\varphi, \theta, \psi)\boldsymbol{v}_r \tag{4}$$

We have as well $\quad \boldsymbol{p}_a - \boldsymbol{m}_a = -R_{euler}(\varphi, \theta, \psi)\cdot\boldsymbol{m}_r$ (5)

By derivating the last equation, we get

$$\boldsymbol{v}_a = -\dot{R}_{euler}\cdot\begin{pmatrix} m_r^x \\ m_r^y \\ m_r^z \end{pmatrix} - R_{euler}\cdot\begin{pmatrix} \dot{m}_r^x \\ \dot{m}_r^y \\ \dot{m}_r^z \end{pmatrix} \tag{6}$$

i.e. $\begin{pmatrix} \dot{m}_r^x \\ \dot{m}_r^y \\ \dot{m}_r^z \end{pmatrix} = -R_{euler}^T\dot{R}_{euler}\cdot\begin{pmatrix} m_r^x \\ m_r^y \\ m_r^z \end{pmatrix} - \boldsymbol{v}_r = f_b\left(m_r^x, m_r^y, m_r^z, \boldsymbol{v}_r, \varphi, \theta, \psi, \dot{\varphi}, \dot{\theta}, \dot{\psi}\right)$ (7)

Moreover in the mobile reference frame the target is located by means of the following equations (see Fig. 1):

$$\begin{cases} \left(m_r^x\right)^2 + \left(m_r^y\right)^2 + \left(m_r^z\right)^2 = d^2 \\ m_r^y = \tan\delta_0.m_r^x = \tan\delta.d \\ -\sin\theta.m_r^x + \cos\theta.\sin\varphi.m_r^y + \cos\theta.\cos\varphi.m_r^z = h \end{cases} \tag{8}$$

We can show that: $\quad a_1\left(m_r^x\right)^2 + b_1 m_r^x + c_1 = 0$ (9)

with $\begin{cases} a_1 = \left[1 + \left(\dfrac{\sin\theta}{\cos\theta\cdot\cos\varphi}\right)^2\right] \\ b_1 = 2\dfrac{\sin\theta}{\cos\theta\cdot\cos\varphi}(h - \cos\theta\cdot\sin\varphi\cdot\tan\delta\cdot d) \\ c_1 = \left(\tan^2\delta - 1\right)\cdot d^2 + \left(\dfrac{h - \cos\theta\cdot\sin\varphi\cdot\tan\delta\cdot d}{\cos\theta\cdot\cos\varphi}\right)^2 \end{cases}$ (10)

and deduce that

$$
\begin{pmatrix} m_r^x \\ m_r^y \\ m_r^z \end{pmatrix} = \begin{pmatrix} \dfrac{-b_1 + \sqrt{\Delta_1}}{2a_1} \\ \tan\delta \cdot d \\ \dfrac{h + \sin\theta\left(\dfrac{-b_1 + \sqrt{\Delta_1}}{2a_1}\right) - \cos\theta \cdot \sin\varphi \cdot \tan\delta \cdot d}{\cos\theta \cdot \cos\varphi} \end{pmatrix} \quad \text{i.e.} \quad \begin{pmatrix} m_r^x \\ m_r^y \\ m_r^z \end{pmatrix} = f_a\begin{pmatrix} d \\ \delta \end{pmatrix} \tag{11}
$$

where $\quad \Delta_1 = b_1^2 - 4a_1 c_1$ \hfill (12)

By derivating (3), we obtain:

$$
\begin{pmatrix} \dot{x}_e \\ \dot{y}_e \end{pmatrix} = \begin{bmatrix} \dfrac{1}{ddist}\sin\left(\dfrac{\delta}{dtheta}\right) & \dfrac{d}{ddist}\dfrac{1}{dtheta}\cos\left(\dfrac{\delta}{dtheta}\right) \\ \dfrac{-1}{ddist}\cos\left(\dfrac{\delta}{dtheta}\right) & \dfrac{d}{ddist}\dfrac{1}{dtheta}\sin\left(\dfrac{\delta}{dtheta}\right) \end{bmatrix}\begin{pmatrix} \dot{d} \\ \dot{\delta} \end{pmatrix} \quad \text{i.e.} \quad (\dot{x}_e, \dot{y}_e) = f_d\left(d,\delta,\dot{d},\dot{\delta}\right) \tag{13}
$$

where $\left(\dot{d}, \dot{\delta}\right)$ can be derived from (8):

$$
\begin{cases} \dot{d} = \dfrac{\dot{m}_r^x . m_r^x + \dot{m}_r^y . m_r^y + \dot{m}_r^z . m_r^z}{d} \\[2mm] \dot{\delta} = \dfrac{\dot{m}_r^y - \dfrac{\tan\delta}{d}.\left(\dot{m}_r^x . m_r^x + \dot{m}_r^y . m_r^y + \dot{m}_r^z . m_r^z\right)}{\left(1 + \tan^2\delta\right)d} \end{cases} \quad \text{i.e.} \quad \left(\dot{d},\dot{\delta}\right) = f_c\left(\dot{m}_r^x, \dot{m}_r^y, \dot{m}_r^z, d, \delta\right) \tag{14}
$$

Given (13), (3), (14), (7) and (11), we can now give the expression of the process model on which our theoretical optical flow is based:

$$
(\dot{x}_e, \dot{y}_e) = f\left(x_e, y_e, \mathbf{v}_r, \varphi, \theta, \psi, \dot{\varphi}, \dot{\theta}, \dot{\psi}\right), \text{ where } f = f_d \, og^{-1} of_c of_b of_a \tag{15}
$$

4. RESULTS

4.1. Detection step (Initialization step of a future Kalman filtering)

A degrading physical effect that appears on sonar images is the speckle noise. This noise is multiplicative if we consider the image as the visualisation of the amplitude modulus of the reflected wave which follows a Rayleigh law [7]. Under this hypothesis, we have derived a simple adjustment test that only consists in verifying the relation of proportionality that exists between the mean and the standard deviation of pixels [8]. In practice, we divide the sonar image into smaller images and test for each of them the value of the ratio between the standard deviation value and mean value of pixels levels. If this ration is too far from the expected value (about 0.52) we consider that a target is in sight. A detected point is the centre of inertia of a set of connected small images whose pixels do not follow a Rayleigh distribution.

4.2. Optical flows

We give in this section a comparison between theoretical flow and observed flow. On the one hand, theoretical flow that we will use later in the prediction step of a Kalman

filtering is based on the previous developed process model. On the other hand, the observed flow is based on the correlation of small images that surround the detected object echo on two successive pings. An example of correlation is given Fig. 2 on the sequence of FLS images where we can see a moored mine in sight.
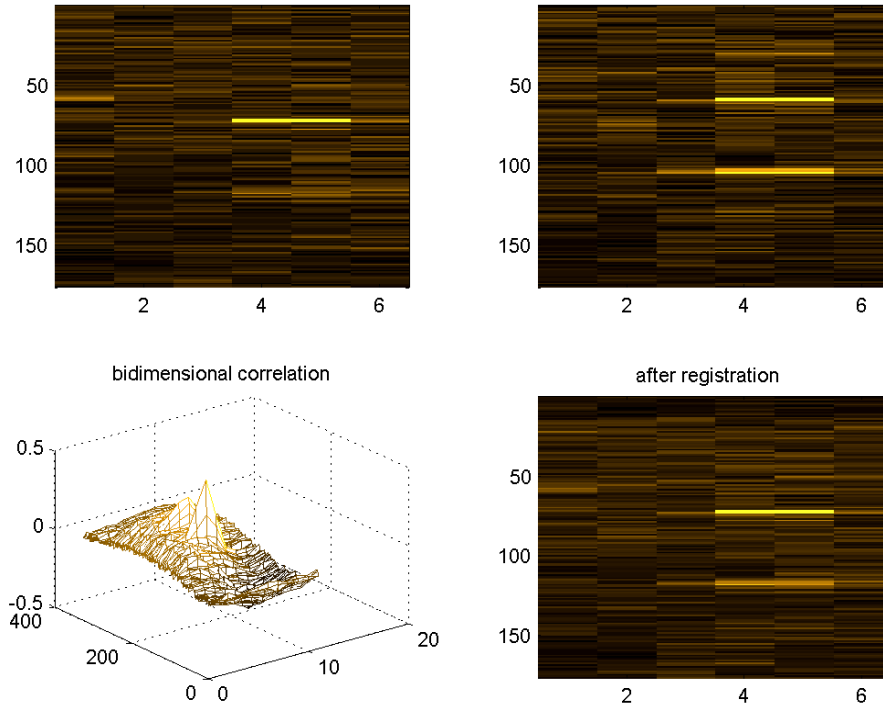

Fig. 2 : results of the correlation of two small images of the detected moored mine

In order to quantitatively compare the two optical flows, we plot the difference between the two related estimated motions versus each ping. Fig. 3 shows on the left a sector image extracted from the sequence with a moored mine in sight (echoes are surrounded in yellow). The two flows (green: observed, red: theoretical) are plotted (with a larger displacement to be visible). On the right we can see the small difference between the estimated motions and that, in spite of the fact that a moored mine is considered. Actually here the tether is too short in relation to the AUV altitude to make the algorithm fail. Another example is given Fig.4 for the shipwreck. Despite these small differences, the observed flow is not reliable because of the poor contrast of these images that leads to a great risk of mistakes in terms of correlation. Lastly theoretical flow is finer than the observed one, i.e. displacement estimation can be finer than the pixel resolution.
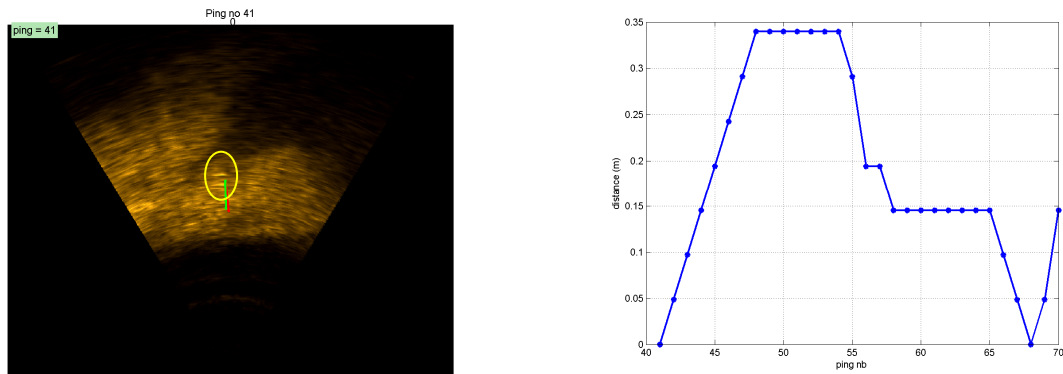

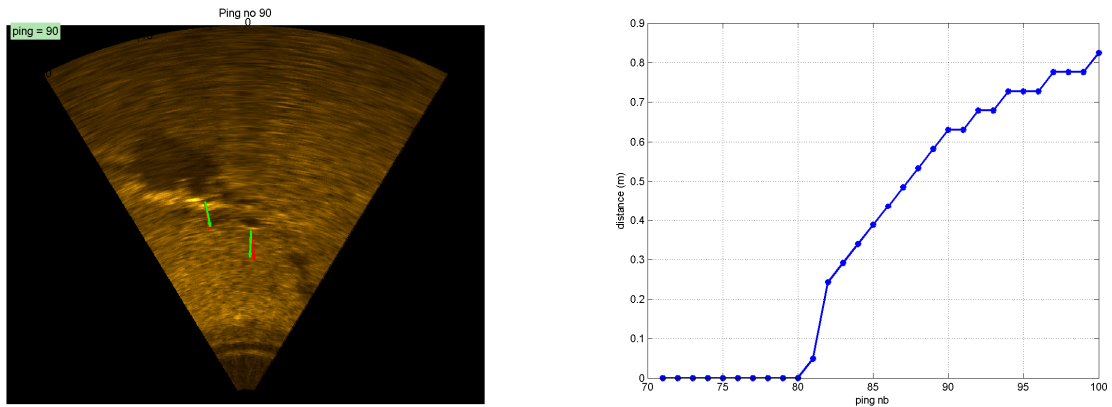*Fig. 3 : Comparison of the two optical flows in the case of moored mine detection*

Fig. 4 : Comparison of the two optical flows in the case of shipwreck detection

5. CONCLUSION

In this article a process model has been developed in order to start with a robust target tracking in an underwater environment. This model is derived from the vehicle process model based on navigation data. It has been tested on real data supplied by the French organism GESMA. First results are encouraging and sufficient to carry on with the development of a Kalman filtering, in progress today.

REFERENCES

[1] **C.D. Loggins**, "A comparison of forward-looking sonar design alternatives", *Proc. of MTS/IEEE Oceans'01*, Honolulu, Hawaii, USA, pp. 1536-1545, 2001.

[2] **F. Devie, J. Lemaire, G. Mailfert & N. Toumelin**, «Developments in the AUV field and description of REDERMOR », *Proc. of the Ninth International Offshore and Polar Engineering Conference*, Brest, France, May 30 – June 4, 1999.

[3] **J. Lemaire & N. Toumelin**, "New capabilities of the REDERMOR Unmanned Underwater Vehicle", *Proc. of MTS/IEEE Oceans' 01*, pp. 380-389, Honolulu, Hawaii, USA, 2001.

[4] **H. Ayreault, V. Lamarre and D. Bouchaud**, "Un Nouveau AUV Experimental pour des Etudes de REA", *Proc. of CMM'06 conference, Sea Tech Week 2006*, Brest, October 2006.

[5] **L. Jaulin**, *Représentation d'état pour la modélisation et la commande de systèmes*, Hermès Lavoisier, 2005.

[6] **T.I. Fossen**, *Guidance and control of ocean vehicles*, Wiley J., 1994.

[7] **F. Schmitt, L. Bonnaud and C. Collet**, „Contrast control for sonar pictures", *Signal and Image Processing, SPIE'96 – Technical Conference on Application of Digital Image Processing XIX*, 2847:70-82, August 1996.

[8] **I. Quidu and Y. Dupas, "**Nouveau test simple d'ajustement à la loi de Rayleigh : application à la détection d'anomalie statistique dans une image sonar », *colloque GRETSI'09*, Dijon, France, 8-11 September 2009, *submitted*.